1972, p 69.
(14) F. Jensen and G. Goodman in "Friedel-Crafts and Related Reactions", Vol. VIII, part 2, G. Olah, Ed., Interscience, New York, N.Y., Chapter 36, p 1003.
(15) F. Reindell and W. Hoppe, *Chem. Ber.*, **87**, 1103 (1954).
(16) A. R. Battersby and J. C. Robinson, *J. Chem. Soc.*, 2076 (1956); A. R. Battersby and J. J. Reynolds, *ibid.*, 524 (1961).
(17) S. Sakakibara in "Chemistry and Biochemistry of Amino Acids, Peptides and Proteins", Vol. I, B. Weinstein, Ed., Marcel Dekker, New York, N.Y., 1971, Chapter 3.
(18) B. W. Erickson and R. B. Merrifield, *J. Am. Chem. Soc.*, **95**, 3757 (1973).
(19) R. S. Feinberg and R. B. Merrifield, *Tetrahedron*, **28**, 5865 (1972).
(20) R. S. Feinberg and R. B. Merrifield, *Tetrahedron*, **30**, 3209 (1974).
(21) B. F. Gisin, *Helv. Chim. Acta*, **56**, 1476 (1973).
(22) B. F. Gisin, *Anal. Chim. Acta*, **58**, 248 (1972).
(23) G. W. Anderson, J. E. Zimmerman, and F. M. Callahan, *J. Am. Chem. Soc.*, **86**, 1839 (1964).

Valence Electron Distribution in Perdeuterio-α-glycylglycine. A High-Resolution Study of the Peptide Bond

Jane F. Griffin* and Philip Coppens

Contribution from the Chemistry Department, State University of New York at Buffalo, Buffalo, New York 14214. *Received February 18, 1975*

Abstract: Carefully collected room temperature X-ray data on perdeuterio-α-glycylglycine have been combined with existing neutron data to give the time-averaged molecular valence and deformation electron densities with an estimated standard deviation of 0.08 e Å^{-3}. The maps presented give a clear indication of bonding effects in the glycylglycine molecule. The density in the peptide C–N bond is elongated perpendicular to the peptide plane, in agreement with the partial double bond character of this bond. Intramolecular effects may be responsible for the asymmetry of the density in the carboxyl group and the polarization of the charge cloud on the peptide oxygen toward the ammonio group. There is no build up of density at the midpoints of the hydrogen bonds, in agreement with the electrostatic model for this interaction. Net charges on the COO^- and NH_3^+ groups are about -0.4 to -0.5 and $+0.4$ electrons, respectively. A refinement on the shape of the atomic valence shell functions indicates the carbon atom to be contracted and the oxygen atom to be expanded relative to the isolated atom functions.

In recent years accurate diffraction techniques have been developed for the direct measurement of the electron distribution in solids. The most informative maps are obtained by a combination of X-ray and neutron diffraction data,[1,2] but qualitative information, especially in the bond regions of the molecules, can also be derived from modified treatments of the X-ray data alone.[3]

In the present study carefully collected room-temperature X-ray data on perdeuterio-α-glycylglycine are combined with the results of a rerefinement of the neutron measurements of Freeman et al.[4] The molecule has been the subject of two recent theoretical studies[5,6] and is of considerable importance because it contains the functional groups characteristic of all proteins. Of special interest are the electronic structure of the peptide bond, the amount and nature of the charge separation in the zwitterion, and the effect of hydrogen bonding on the electron distribution.

The geometry of the molecule has been discussed in earlier publications[4,7] and will therefore not be treated here.

Experimental Section

X-Ray Data Collection and Reduction. Crystals of perdeuterio-α-glycylglycine were kindly supplied by Drs. G. L. Paul and T. M. Sabine. A moderately well-formed crystal, roughly parallelepiped-shaped, 0.25 mm on edge was selected. The unit cell used by previous authors was transformed to a unit cell in space group $P2_1/c$ with a β angle of 107.656°. The cell constants, listed in Table I together with earlier values, were obtained by a least-squares refinement[8] of the setting angles of 18 reflections with $30° < 2\theta < 63°$. Data were collected on a Picker automated diffractometer using Zr filtered Mo Kα radiation. Three standard reflections were measured at regular intervals and used to scale the data. Integrated intensities were obtained by analysis of the reflection profiles using a technique described recently[9] and corrected for absorption (μ = 1.87 cm^{-1}) by Gaussian numerical integration. The 6382 measured reflections were symmetry-averaged to give 3590 independent reflections for the least-squares input; of these 2257 are at sin $\theta/\lambda > 0.65$ Å^{-1}. Discrepancies between symmetry-related reflections agree well with counting statistics and average less than 1.5% for the 1100 strongest reflections. All programs used for data reduction and refinement are part of the Integrated Crystallographic Computing Library at the State University of New York at Buffalo.

X-Ray Data Refinement. Neutron parameters were used as input in the full matrix least-squares minimization of $\Sigma w (F_{obsd}^2 - k^2F_{calcd}^2)^2$ in which $w = 1/\sigma^2$ and $\sigma^2 = \sigma^2_{counting} + (0.03F_{obsd}^2)^2$. Reflections for which $F_{obsd}^2 < 3\sigma(F_{obsd}^2)$ were included only if $F_{calcd}^2 > 3\sigma(F_{obsd}^2)$, in which case F_{obsd}^2 was taken as $3\sigma(F_{obsd}^2)$. Atomic scattering factors used were as listed in Volume 4 of the International Tables for X-ray Crystallography (C, N, O) and, for hydrogen, as given by Stewart et al.[10] A preferable refinement in which all measured reflections were included[11a] yielded positional and thermal parameters within one standard deviation from those listed in Table II. However, the direction of the differences is systematic as predicted by Hirshfeld and Rabinovich;[11a] the thermal parameters from the alternative refinement are larger than those from the previous treatment. In all refinements an isotropic extinction parameter was included as a variable.[11b] For a table of final X-ray structure factors, see ref 12. Agreement factors are summarized in Table III.

Neutron Data Refinement. In the neutron refinement by Freeman et al.[4] strong correlations were encountered between several parameters. In the rerefinement, these correlations were avoided by the transformation to the new cell, with a β angle closer to 90°. In this way correlation coefficients, except those between the scattering length and thermal parameters of the deuterium atoms, were reduced to values less than 0.5. The function minimized was $\Sigma w (F_{obsd} - kF_{calcd})^2$ with $w = 1/\sigma^2 = (4.0 + F_o + 0.013F_o^2)^{-1}$. The constants in this expression were chosen such that the first two terms dominated for weak reflections, while the third term prevented assignment of too high a weight to the strong reflections. A number of extinction-affected reflections were omitted from the

* Address correspondence to this author at the Medical Foundation of Buffalo, Buffalo, New York 14203.

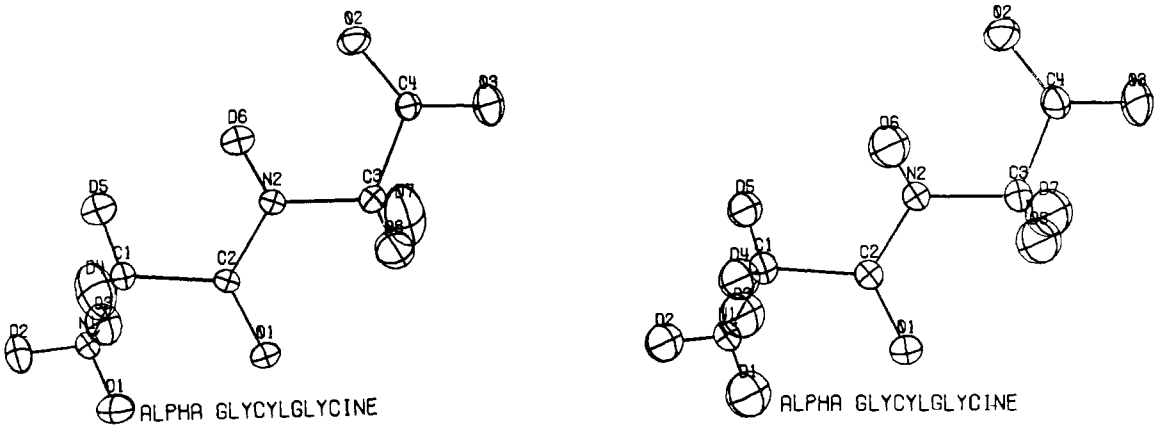

Figure 1. ORTEP drawing of 50% probability thermal ellipsoids of α-glycylglycine: left, parameters from neutron refinement; right, parameters from conventional X-ray refinement.

Table I. Cell Constants

	Hughes[a]	Free-man[b,c]	Freeman transformed	Present study[c]
a, Å	7.812 (2)	9.4251 (2)	8.1105	8.1232 (8)
b, Å	9.566 (3)	9.5586 (6)	9.5586	9.5589 (8)
c, Å	9.410 (3)	7.8271 (3)	7.8271	7.8250 (9)
β, deg	124.60 (2)	124.853 (2)	107.516	107.656 (6)
Space group	$P2_1/a$	$P2_1/c$	$P2_1/c$	$P2_1/c$
Z	4	4	4	4
Formula wt	132.1	140.2	140.2	140.2
Vol, Å^3	578.82	578.66	578.66	578.98
d_X	1.512	1.606		1.606

[a] E. A. Hughes, *Acta Crystallogr., Sect. B*, 24, 1128 (1968). [b] H. C. Freeman, G. L. Paul, and T. M. Sabine, *Acta Crystallogr., Sect. B*, 26, 925 (1970). [c] Perdeuterio.

published structure factor list of Freeman et al.[4] and were therefore excluded from the rerefinement. Neutron scattering lengths used for C, N, O, D, and H were 0.6648, 0.9140, 0.5803, 0.6672 and -0.374×10^{-12} cm, respectively.[13] The scattering length of hydrogen was treated as an additional variable to allow for partial deuteration. The D/H ratios found are in substantial agreement with those reported by Freeman et al.[4] and vary between 96 and 100%. The new structural parameters differ only slightly from the earlier values (Table II).

Results and Discussion

Comparison of X-Ray and Neutron Positional Parameters. Agreement between the positional parameters from the X-ray refinements (full data and high angle) and from the neutron experiment is generally good. Slight differences are found for the oxygen atoms. The carbonyl oxygen position when determined with X-rays is displaced into the C(2)-O(1) region by 0.007 (3) Å, while the O(2) and O(3) atoms of the carboxyl group are displaced toward their lone pairs by 0.004 (3) and 0.007 (3) Å, respectively.

These shifts are similar in magnitude to those observed in other comparative X-ray and neutron diffraction studies[1] and are attributed to the asphericity of the atomic charge cloud due to bonding effects. However, in the present study the discrepancies are barely significant when compared to the standard deviations, which are dominated by the error estimates in the neutron parameters.

Figure 1 is a graphic representation of the thermal vibrational parameters (50% probability ellipsoids) as determined by neutron and X-ray refinement. The X-ray ellipsoids show the bias due to the sperical-atom approximation used in the refinement.[14] They are generally larger than the neutron ellipsoids and often extended into bonds with appreciable overlap density: C(1) into the C(1)-D(5) bond, C(4) into the C(4)-O(2) bond, and C(2) into the C(2)-O(1) bond (see Figures 1 and 10 for labeling of atoms).

Definition of Difference Densities. In the analysis of electron density distributions, it is convenient to examine difference density functions which reveal the effects of chemical bonding more readily. We shall employ two types of difference densities

(a) valence density

$$\rho_{\text{valence}}(\mathbf{r}) = \frac{1}{V}\sum_{\mathbf{H}}[F_{\text{obsd}}(\mathbf{H}) - F_{\text{core}}(\mathbf{H})]^{-2\pi i\mathbf{H}\cdot\mathbf{r}}$$

(b) deformation density

$$\rho_{\text{deformation}}(\mathbf{r}) = \frac{1}{V}\sum_{\mathbf{H}}[F_{\text{obsd}}(\mathbf{H}) - F_{\text{spherical atom}}(\mathbf{H})]^{-2\pi i\mathbf{H}\cdot\mathbf{r}}$$

where H and **r** are the reciprocal lattice vector and a vector in crystal space, respectively, and V is the volume of the unit cell.

The first summation represents the distribution of the valence electrons using the assumption that the core electrons are unperturbed by bonding effects, a limitation which seems well justified within the resolution of the diffraction experiment.[15] The second summation more commonly used in crystallography corresponds to the deformation of the electron density of the pro molecule (i.e., the assembly of spherical atoms placed at the atomic positions) upon molecule formation. For both summations unbiased estimates of the nuclear coordinates and thermal vibration parameters are desirable. They are preferably obtained from an independent neutron experiment (ρ_{X-N}), though qualitative information can also be extracted with parameters from high-order X-ray refinements (ρ_{X-X}).[3] A comparison of Figures 2a and 3a with 2b and 3b shows the enhanced detail of the X-N maps, especially in the lone pair regions. The functions ρ_{X-N} will therefore be used here as basis for the discussion.

Both valence and deformation densities will be examined. It is especially the latter which can reveal sensitive details of the charge distribution, such as the accumulation of charge in bonding and lone pair regions.

The average standard deviation in the difference functions, estimated as described earlier, is 0.08 e Å^{-3}.[1] Errors are larger in the regions of the nuclei where especially the height and, to a much smaller extent, the shape of the function are affected by the choice of scale factor. The accuracy of the present study is mainly limited by the neutron experiment, which should be repeated if further detail becomes desirable.

Table II. Structure Parameters

		Atomic coordinates			Thermal parameters[b]					
		x	y	z	U_{11}	U_{22}	U_{33}	U_{12}	U_{23}	U_{13}
C(1)	A[a]	−0.3429 (2)	0.0953 (2)	−0.1034 (3)	219 (8)	161 (7)	183 (7)	−12 (5)	−23 (6)	17 (5)
	B	−0.3430 (2)	0.0951 (2)	−0.1029 (3)	222	171	169	−19	−18	25
	C	−0.3430 (2)	0.0957 (2)	−0.1034 (2)	235 (5)	220 (4)	215 (4)	−16 (4)	−15 (4)	24 (4)
	D	−0.3434 (1)	0.0953 (1)	−0.1032 (1)	216 (4)	205 (4)	197 (4)	−14 (3)	−22 (3)	22 (3)
C(2)	A	−0.4853 (2)	0.1708 (2)	−0.2428 (2)	199 (7)	125 (7)	180 (7)	−18 (7)	−23 (6)	−18 (5)
	B	−0.4854 (2)	0.1705 (2)	−0.2431 (3)	194	120	189	−8	−18	−7
	C	−0.4851 (2)	0.1709 (1)	−0.2435 (2)	208 (4)	187 (4)	207 (4)	1 (4)	−11 (3)	−14 (3)
	D	−0.4855 (1)	0.1709 (1)	−0.2435 (1)	190 (4)	167 (3)	191 (4)	1 (3)	−5 (3)	−14 (3)
C(3)	A	−0.7665 (3)	0.1553 (2)	−0.4666 (3)	257 (8)	154 (7)	315 (9)	33 (6)	−83 (7)	−35 (6)
	B	−0.7659 (2)	0.1552 (2)	−0.4663 (3)	258	167	296	30	−85	101
	C	−0.7663 (3)	0.1557 (2)	−0.4662 (3)	262 (5)	217 (5)	335 (5)	46 (4)	−89 (4)	−36 (4)
	D	−0.7666 (2)	0.1556 (1)	−0.4664 (2)	244 (4)	205 (4)	318 (5)	45 (3)	−92 (4)	−37 (3)
C(4)	A	−0.8616 (2)	0.0536 (2)	−0.6111 (2)	213 (7)	164 (7)	144 (7)	−3 (5)	−19 (6)	15 (5)
	B	−0.8617 (2)	0.0538 (2)	−0.6114 (3)	212	176	146	−8	−12	14
	C	−0.8619 (2)	0.0536 (2)	−0.6104 (2)	216 (4)	245 (4)	189 (4)	−16 (4)	13 (3)	15 (3)
	D	−0.8614 (1)	0.0553 (1)	−0.6105 (1)	195 (4)	223 (4)	170 (3)	−12 (3)	8 (3)	15 (3)
N(1)	A	−0.1778 (2)	0.1690 (1)	−0.0769 (2)	203 (6)	168 (6)	174 (6)	4 (4)	−22 (5)	−10 (4)
	B	−0.1779 (2)	0.1694 (1)	−0.0768 (2)	212	180	189	0	−26	18
	C	−0.1781 (2)	0.1692 (2)	−0.0770 (2)	215 (4)	216 (4)	218 (4)	−2 (3)	−29 (3)	−18 (3)
	D	−0.1781 (1)	0.1691 (1)	−0.0769 (1)	194 (3)	195 (4)	196 (3)	−2 (3)	−35 (2)	−16 (3)
N(2)	A	−0.6179 (2)	0.0932 (1)	−0.3364 (2)	217 (6)	136 (5)	235 (6)	−13 (4)	−49 (5)	−6 (4)
	B	−0.6179 (2)	0.0934 (1)	−0.3363 (2)	228	144	256	−4	−47	−4
	C	−0.6178 (2)	0.0927 (1)	−0.3362 (2)	230 (4)	167 (4)	280 (4)	0 (3)	−56 (3)	−4 (3)
	D	−0.6175 (1)	0.0934 (1)	−0.3362 (1)	211 (4)	155 (3)	264 (4)	−2 (2)	−61 (3)	−6 (3)
O(1)	A	−0.4787 (3)	0.2991 (2)	−0.2612 (4)	317 (11)	128 (9)	378 (12)	−5 (7)	−80 (9)	−7 (8)
	B	−0.4788 (3)	0.2989 (2)	−0.2610 (4)	319	106	391	−11	−79	0
	C	−0.4778 (3)	0.2989 (1)	−0.2618 (3)	332 (4)	174 (3)	414 (5)	−19 (3)	−76 (4)	−2 (3)
	D	−0.4781 (1)	0.2986 (8)	−0.2614 (1)	297 (4)	139 (3)	381 (4)	−20 (2)	−84 (3)	−2 (2)
O(2)	A	−0.8216 (3)	−0.0735 (2)	−0.5910 (3)	382 (11)	156 (9)	178 (8)	−25 (7)	−8 (8)	−10 (6)
	B	−0.8220 (3)	−0.0736 (2)	−0.5907 (4)	382	153	197	−19	0	−14
	C	−0.8227 (3)	−0.0735 (2)	−0.5907 (2)	412 (5)	209 (4)	235 (4)	−14 (3)	9 (3)	−16 (3)
	D	−0.8220 (1)	−0.0733 (8)	−0.5911 (1)	377 (4)	179 (3)	201 (3)	−14 (2)	0 (2)	−14 (2)
O(3)	A	−0.9734 (4)	0.1065 (4)	−0.7396 (4)	395 (13)	372 (13)	224 (11)	28 (10)	−131 (10)	50 (9)
	B	−0.9736 (3)	0.1069 (3)	−0.7401 (5)	376	370	245	45	−123	43
	C	−0.9746 (4)	0.1068 (3)	−0.7396 (3)	429 (5)	447 (5)	277 (4)	68 (4)	−137 (4)	49 (4)
	D	−0.9736 (1)	0.1059 (1)	−0.7402 (1)	402 (5)	410 (5)	244 (4)	64 (3)	−141 (3)	50 (3)
D(1)	A	−0.1927 (3)	0.2748 (2)	−0.0576 (4)	235 (12)	194 (11)	448 (14)	−40 (7)	5 (9)	−45 (8)
	B	−0.1925 (3)	0.2744 (2)	−0.0582 (4)	340	185	434	−22	12	−14
	C	−0.1867	0.2625	−0.0549	454					
	D	−0.1867 (2)	0.2625 (2)	−0.0549 (2)	454 (48)					
D(2)	A	−0.0873 (3)	0.1335 (2)	0.0390 (3)	268 (11)	332 (12)	271 (11)	50 (7)	−68 (7)	4 (8)
	B	−0.0879 (3)	0.1336 (2)	0.0391 (3)	258	301	293	−41	−67	−22
	C	−0.0982	0.1365	0.0288	319					
	D	−0.0982 (2)	0.1365 (2)	0.0288 (2)	319 (37)					
D(3)	A	−0.1363 (3)	0.1529 (3)	−0.1877 (3)	356 (13)	458 (15)	325 (13)	−3 (9)	85 (9)	24 (9)
	B	−0.1366 (3)	0.1529 (3)	−0.1877 (3)	340	417	301	−11	88	7
	C	−0.1400	0.1524	−0.1806	511					
	D	−0.1400 (3)	0.1524 (2)	−0.1806 (3)	511 (51)					

D(4)	A	−0.3747 (4)	0.0987 (4)	0.0215 (4)	399 (15)	653 (22)	259 (14)	−38 (11)	76 (10)	110 (10)
	B	−0.3744 (3)	0.0984 (3)	0.0219 (4)	404	653	262	−37	79	123
	C	−0.3748	0.0946	0.0065	324					
	D	−0.3748 (2)	0.0946 (2)	0.0065 (2)	324 (39)					
D(5)	A	−0.3291 (4)	−0.0130 (3)	−0.1396 (4)	417 (14)	213 (12)	499 (16)	−18 (8)	−90 (11)	11 (9)
	B	−0.3299 (3)	−0.0126 (2)	−0.1405 (5)	407	176	510	−4	−70	217
	C	−0.3337	0.0033	−0.1351	259					
	D	−0.3337 (2)	0.0033 (2)	−0.1351 (2)	259 (37)					
D(6)	A	−0.6099 (3)	−0.0130 (2)	−0.3292 (3)	353 (12)	170 (10)	406 (14)	−22 (7)	−59 (9)	2 (7)
	B	−0.6101 (3)	−0.0132 (2)	−0.3294 (4)	378	148	397	−26	−53	0
	C	−0.6104	0.0096	−0.3311	366					
	D	−0.6104 (2)	0.0096 (2)	−0.3311 (2)	366 (46)					
D(7)	A	−0.8564 (5)	0.1946 (5)	−0.4003 (5)	470 (19)	796 (30)	492 (21)	336 (17)	−83 (13)	−377 (19)
	B	−0.8565 (4)	0.1949 (4)	−0.3998 (6)	492	801	502	341	−67	−347
	C	−0.8500	0.1924	−0.4049	429					
	D	−0.8500 (2)	0.1924 (2)	−0.4049 (2)	429 (48)					
D(8)	A	−0.7240 (5)	0.2430 (3)	−0.5311 (6)	576 (22)	315 (16)	739 (26)	−149 (13)	−216 (17)	202 (14)
	B	−0.7244 (4)	0.2436 (3)	−0.5309 (7)	588	292	707	−127	−243	206
	C	−0.7346	0.2337	−0.5207	461					
	D	−0.7346 (2)	0.2237 (2)	−0.5207 (2)	461 (48)					

[a] A = present study neutron refinement described in text. B = Freeman et al. study coordinates transformed into new cell. C = high angle X-ray refinement, deuterium parameters not varied. D = conventional X-ray refinement, deuterium isotropic thermal parameters. [b] The thermal parameters are in 10^{-4} Å^2. The temperature factor used is $T(hkl) = \exp[-2\pi^2(h^2a^{*2}U_{11} + k^2b^{*2}U_{22} + l^2c^{*2}U_{33} + 2hka^*b^*U_{12} + 2klb^*c^* - U_{23} + 2hla^*c^*U_{13})]$.

Choice of Scale Factor. The density in the immediate vicinity of the nuclei is affected appreciably by the choice of scale factor relating the observations to the structure factors calculated on an absolute scale.[16] In several instances the scale factor k, defined as $F_{obsd} = kF_{calcd}$, from a conventional least-squares refinement has been found to be too large by up to 10%. In the study of kernite,[17] the experimentally determined scale factor agreed well with the least-squares value obtained with contracted Slater-type scattering factors. In the present work, a value of 5.90 (1) was obtained in the conventional refinement, while values of 5.54 (1) and 5.62 (3) resulted from a spherical charge refinement in the ELS (extended L shell) approximation, and from a similar refinement which also included an atomic shape parameter (κ refinement, see below) (Table III). The latter value, which is about 5% smaller than the conventional scale factor, was adopted in the calculation of the X-N maps, a choice which is justified a posteriori by the reasonable appearance of the X-N deformation maps. It should be emphasized, however, that the peak heights near the nuclei are sensitive to the choice of scale factor.

The Peptide Bond. Both theoretical[5] and experimental arguments based on bond lengths support the partial double bond character of the C-N bond, even though the peptide group is appreciably distorted from planarity.[18] Thus, a C-N single bond between sp^2 hydridized C and N atoms is about 1.49 Å, while a double bond is about 1.27 Å long. The length of the peptide bond (1.326 Å) is clearly intermediate. Bond peaks are apparent in the section through the N, C, and O atoms (Figure 3). The maximum deformation densities are 0.35 and 0.48 e Å^{-3} in the C-N and C-O (l = 1.238 Å) bonds, respectively. These values may be compared with those obtained in the low-temperature X-N study of cyanuric acid:[19] C-N l = 1.370 Å, ρ_{max} = 0.50 e Å^{-3}; C-O l = 1.216 Å, ρ_{max} = 0.30 and 0.50 e Å^{-3}. The section of the deformation density perpendicular to the C-N bond through its midpoint (Figure 4) clearly shows elongation perpendicular to the peptide plane. Analogous elongations have also been seen in sections perpendicular to the C-C bonds in various hydrocarbons,[20] in unsaturated alcohols,[21] and in tetracyanoethylene,[2] confirming the partial double bond character.

The peak height in the peptide oxygen-lone pair region is unusually small, compared with values of 0.15-0.45 e Å^{-3} observed in other studies.[1] This effect is also evident in the valence density (Figure 5), which peaks slightly *inward* relative to the oxygen nuclear position. It is tempting to attribute this effect to a *through space* polarization of the oxygen charge cloud by the positive charge on the ammonio ($-NH_3^+$) group, as predicted from qualitative arguments by Coulson.[22] Such a charge polarization would also explain the displacement of the C-O overlap density maximum from the bond axis toward the NH_3^+ group in Figure 3.

As observed earlier in an X-X study of uracil[23] the valence density (Figure 5) does not peak at the carbon atoms. Instead, the carbon is close to a saddle point connecting the charge maxima near the oxygen and nitrogen atoms.

The Carboxyl Group. The plane through the carboxyl group (Figure 2a) shows considerable asymmetry in the residual density in the two C-O bonds. The two bonds are similar in length, 1.255 (4) Å and 1.240 (4) Å, but have peak maxima of 0.48 e Å^3, C(4)-O(2), and 0.23 e Å^3, C(4)-O(3) (see Figure 6). Similar lack of symmetry has been observed in X-N deformation maps of carboxyl groups in ammonium tetraoxalate,[24] glycine,[25] and ammonium oxalate monohydrate.[26] Of all these, the present study shows perhaps the most persuasive difference, relative to the noise level in areas away from the molecule. An analysis

Table III. Scale Factors and Residuals from a Number of Refinements[a]

Refinement	Scale factor	NR	NV	NV/NR	$R(F)$, %	$R_w(F)$, %	$R(F^2)$, %	$R_w(F^2)$, %
Neutron	9.80	1679	154		6.8		10.0	
Conventional least squares	5.90 (1)	1956	115	17	4.4	4.7	5.9	9.2
High angle refinement	5.90[b]	903	81	11	5.9	5.3	8.6	10.2
ELS HF core, STO valence, full refinement	5.54 (1)	1962	131	15	4.0	4.2	4.4	8.3
ELS HF core, STO valence, full refinement including parameter	5.62 (3)	1966	135	14.5	3.9	4.1	4.1	8.2

[a] NR = number of reflections, NV = number of parameters. [b] Not varied.

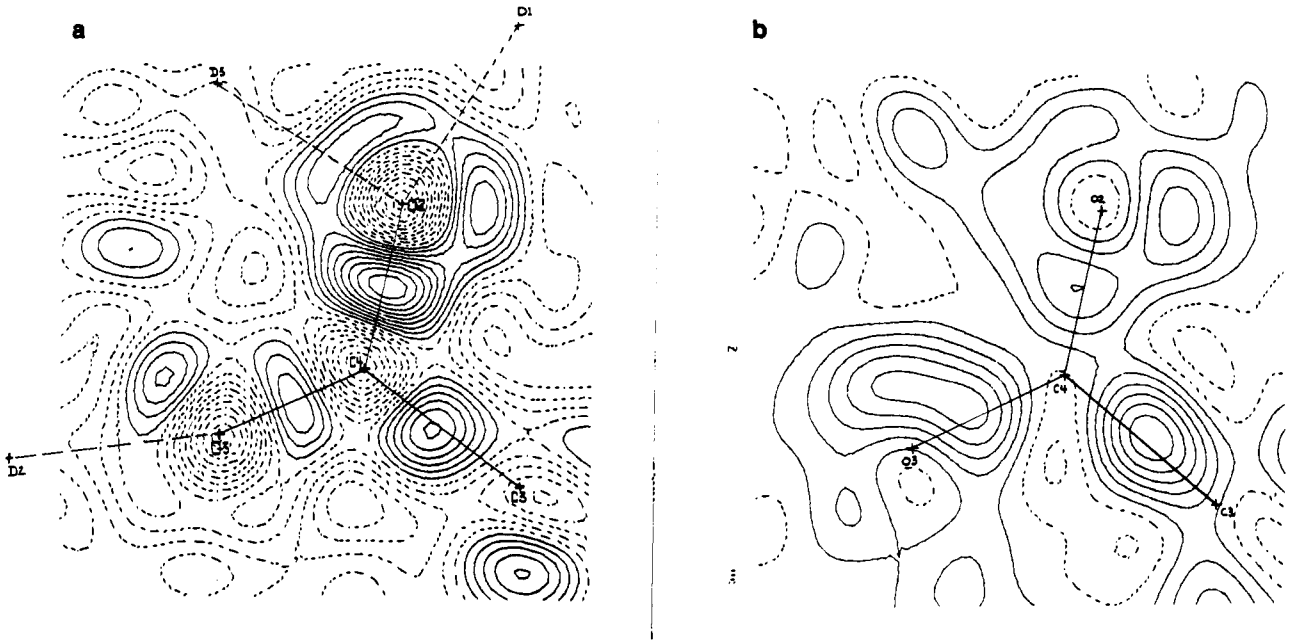

Figure 2. Carboxyl plane defined by C(4)-O(2)-O(3): (a) ρ_{X-N}; (b) ρ_{X-X}. Contours at 0.05 e/Å^3.

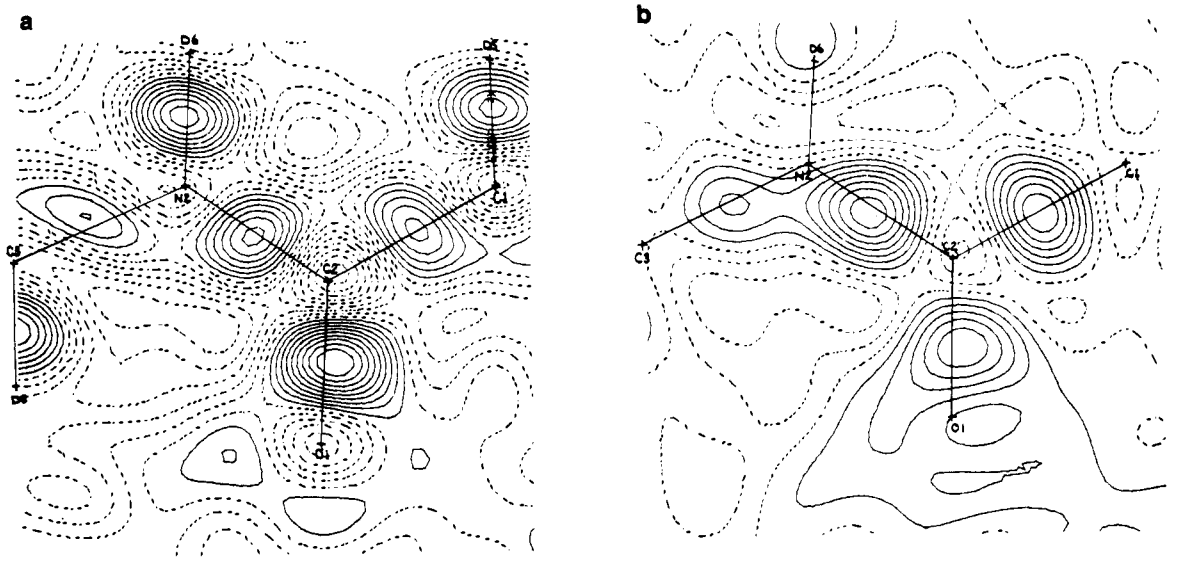

Figure 3. Peptide plane defined by C(2)-O(1)-N(2): (a) ρ_{X-N}; (b) ρ_{X-X}. Contours at 0.05 e/Å^3.

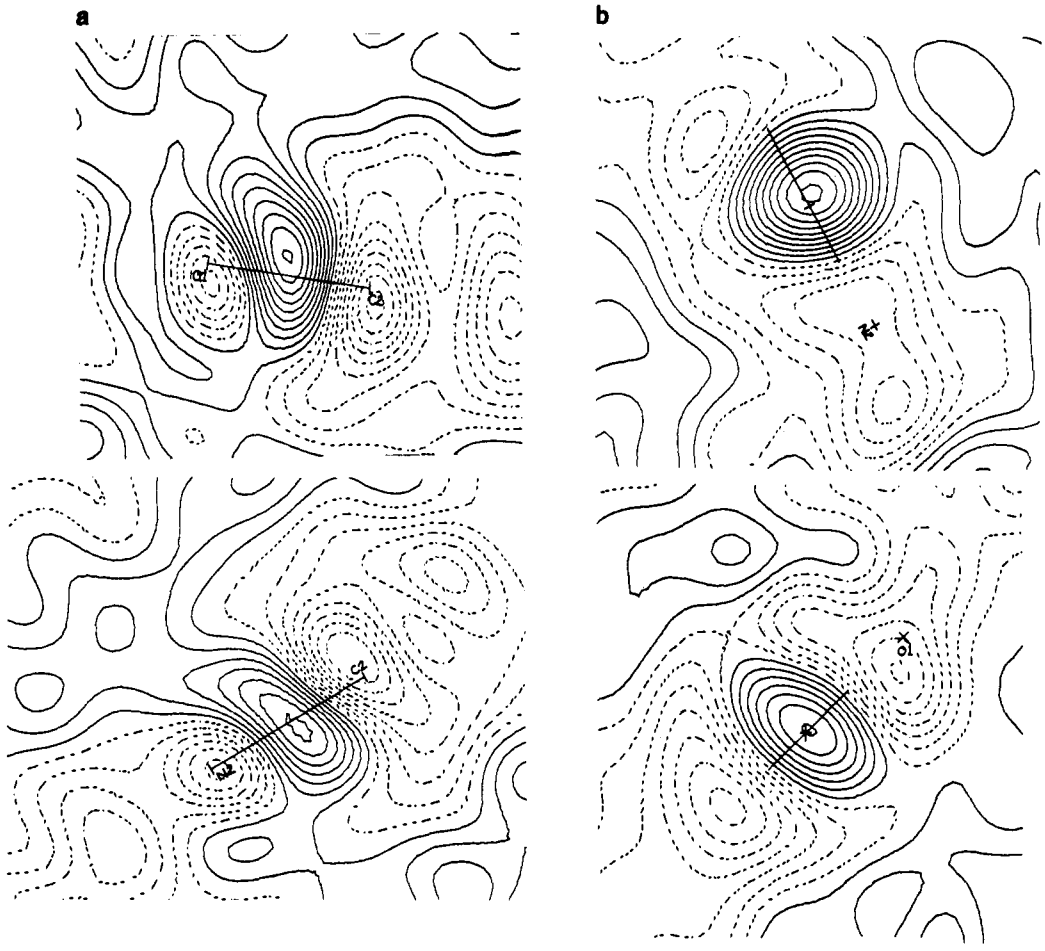

Figure 4. (a) Sections perpendicular to the peptide plane and containing C(2)-O(1) (top) and C(2)-N(2) (bottom). (b) Sections perpendicular to bonds through the midpoint of the bond: C(2)-O(1) (top); C(2)-N(2) (bottom). Contours at 0.05 e/Å^3.

of the peak height dependence on thermal motion, using an approximation developed for tetracyanoethylene,[1] shows that a difference of 0.05-0.10 e Å^3 can be attributed to the larger vibrational amplitude of the O(3) atom (Table II). Thus, a slight polarization of the carboxyl group due to intramolecular effects or to the asymmetry in the hydrogen bonding cannot be ruled out.

The asymmetry of the carboxyl group is also expressed in an apparent absence of a second lone pair on the O(3) atom. A further exploration of the density function around O(3) shows that there is a crescent-shaped slice of density around O(3) in a plane inclined to the plane of the carboxylate group. This can be seen more clearly in Figure 8a, which is a section containing the O(3) and D(2) atoms.

Hydrogen Bonding and the Density in the NH_3^+ Group. Each of the three deuterium atoms of the ammonio, ND_3^+, group participates in a strong hydrogen bond to a carboxyl oxygen of three different carboxyl groups, while the peptide hydrogen is involved in a weaker bond with a peptide carbonyl (Table IV). A detailed discussion of this geometry has been given by Biswas et al.[7] and by Freeman et al.[4]

Difference densities in sections containing O- - -D within and perpendicular to the N-D- - -O planes are given in Figures 7 and 8. Inspection of these maps leads to the following observations.

(a) There is no buildup of density near the midpoint of the deuterium atom and the oxygen acceptor, in accordance with an electrostatic model for the interaction. Similar conclusions have been drawn from theoretical calculations by Kollman and Allen[27] on the H_2O- - -HF complex and by Dreyfus et al.[28] on the cyclic, planar dimer of formamide.

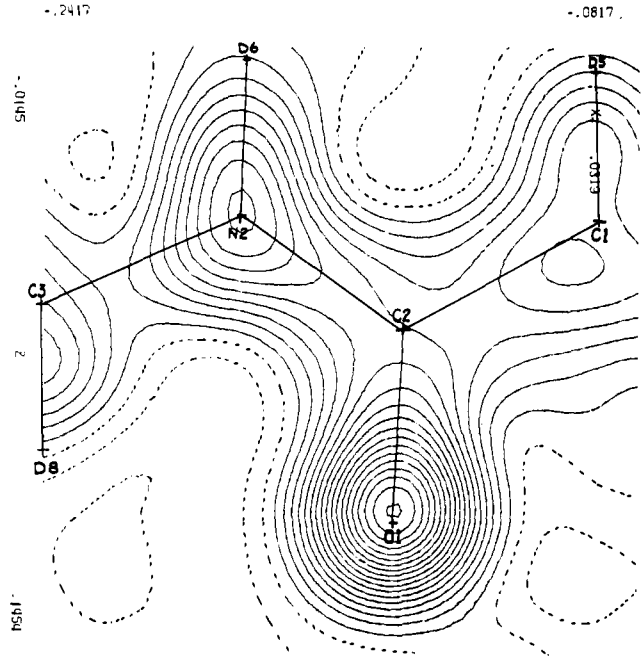

Figure 5. Valence density in the peptide plane. Contours at 0.25 e/Å^3.

Both these calculations indicate a depletion of the density in the hydrogen bond region and an increase of density in the covalent X-H bond. These conclusions are in qualitative agreement with the present experimental results, though, in the absence of a non-hydrogen-bonded N-H group, an in-

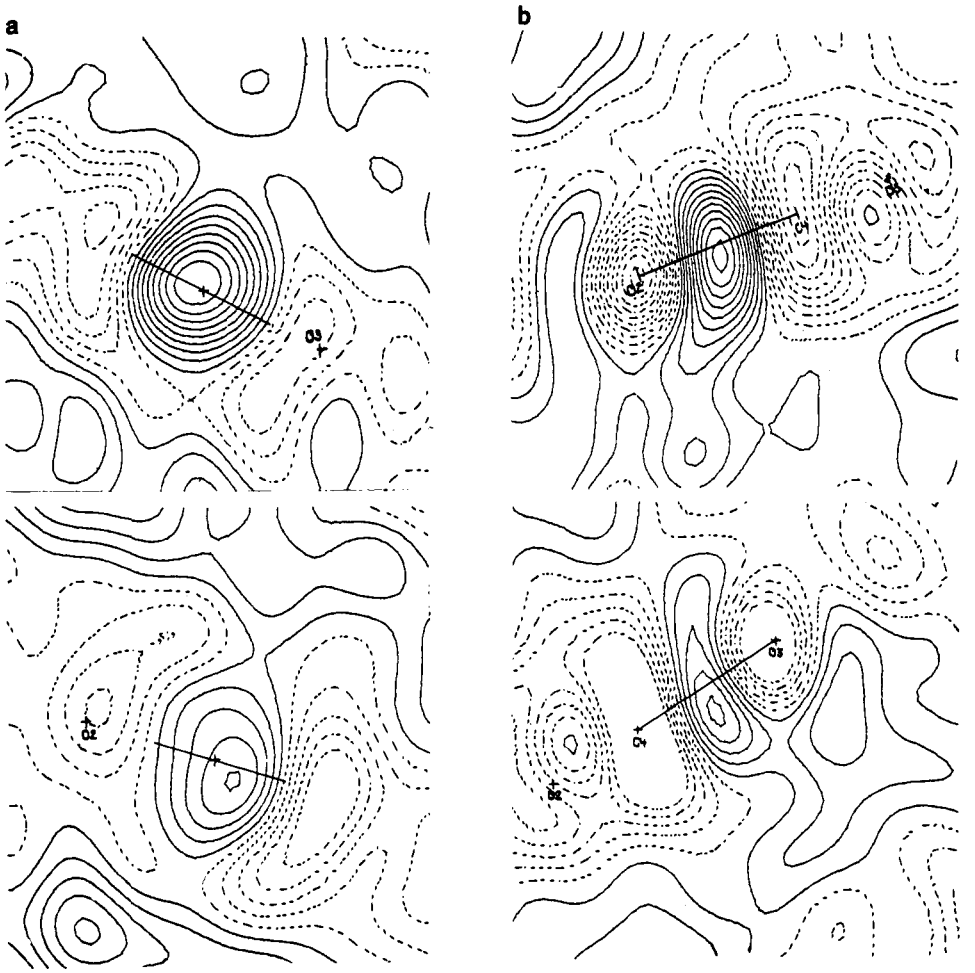

Figure 6. ρ_{X-N}: (a) sections perpendicular to bonds through the midpoint of the bonds C(4)-O(2) (top) and C(4)-O(3) (bottom); (b) section perpendicular to the carboxyl group and containing C(4)-O(2) (top) and C(4)-O(3) (bottom). Contours at 0.05 e/Å^3.

Table IV. Hydrogen Bonds. Bond Distances and Angles

Atoms	N–D, Å	N···O, Å	D···O, Å	N–D···O, deg	D···O–C, deg
N(1)–D(1)···O(2)	1.035 (3)	2.753 (3)	1.840 (3)	150.9 (0.3)	143.7 (0.3)
N(1)–D(2)···O(3)	1.036 (3)	2.724 (3)	1.719 (3)	162.5 (0.3)	156.4 (0.3)
N(1)–D(3)···O(2)	1.033 (3)	2.790 (3)	1.825 (3)	147.5 (0.3)	108.4 (0.3)
N(2)–D(6)···O(1)	1.018 (3)	2.956 (3)	1.983 (3)	158.9 (0.3)	151.5 (0.3)

terpretation of the experimental N–H peak height is necessarily tentative.

(b) There is a tendency for the N–D vectors to point toward the lone-pair density rather than to the center of the acceptor atom (Figure 8). A similar conclusion has been drawn from molecular packing considerations of primary amides by Leiserowitz and Schmidt.[29]

(c) Both Figures 7 and 8 indicate that in all cases, lone-pair density accumulates close to the line connecting D and O atoms (although the maximum may be displaced so as to lie along the extension of N–D as discussed in b above).

The section through D(1), D(2), and D(3), with the positions of N(1), O(2), and O(3) projected onto the plane, is shown in Figure 9. A displacement of deuterium atom density into the N–D covalent bond is evident.

Polarization of the Bond Density. Due to the difference in the number of valence electrons, the valence density shows its maxima at the nitrogen and oxygen but not at the carbon atoms. A further polarization of the density toward the more electronegative atom is observed in the deformation sections through the bonds perpendicular to the molecular planes. Thus, Figure 4 shows the bond maxima in C(2)–O(1) and C(2)–N(2) to be curved toward the more electronegative atom. Similar effects are found in the C(4)–O(3) and C(4)–O(2) bonds (Figure 6b) but not in the C(1)–C(2) and C(4)–C(3) bonds, where none would be expected.

Net Atomic Charges and the Charge Separation in the Zwitterion. Though no distinct atomic entities exist in a molecular crystal, approximate atomic charges may be obtained by least-squares adjustment of the occupancy of atomic density functions together with other structural parameters (ELS refinement).[30,31] A conceptual ambiguity is inherent in the choice of the atomic density functions. In a number of studies optimal agreement with experimental measurements has been obtained by the selection of molecule-optimized Slater type scattering factors[30-32] which in the case of kernite also gave the best agreement with the experimentally determined scale factor.[7] As a similar trend is found in the present study, only the results obtained with Slater-type orbitals (STO) scattering factors will be dis-

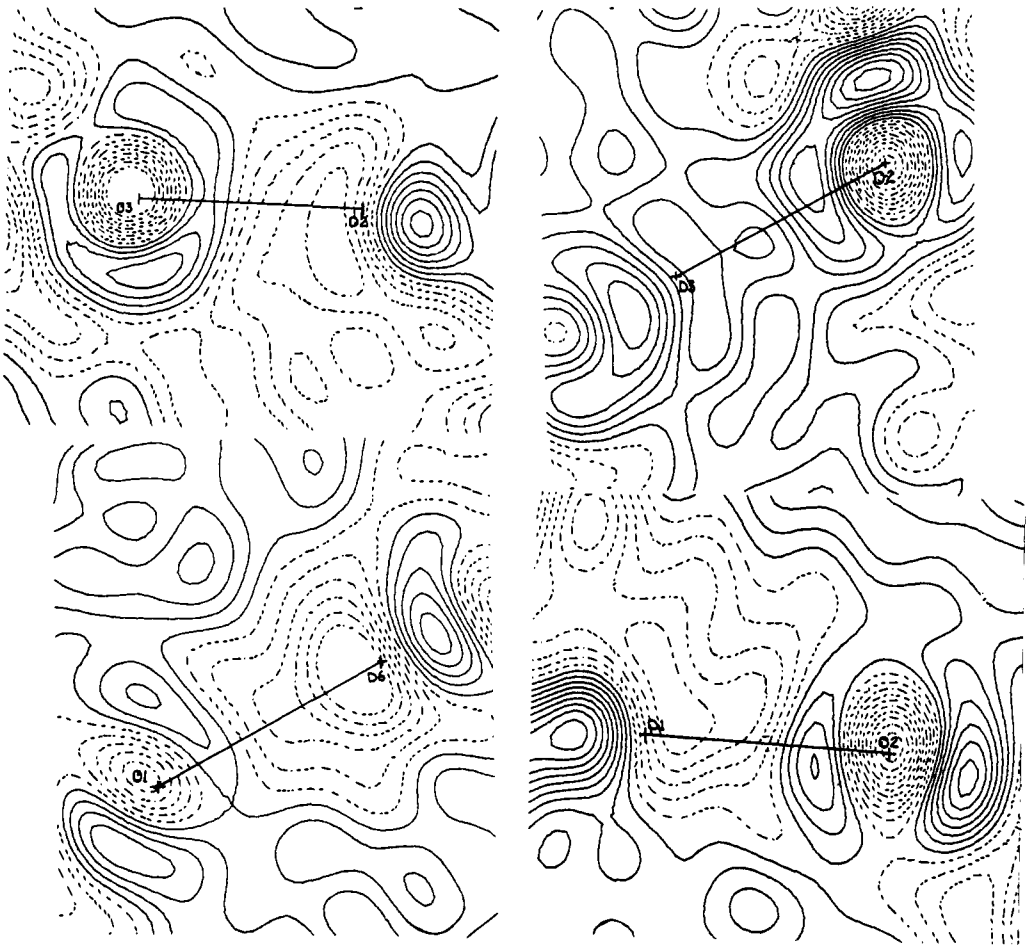

Figure 7. Sections through the planes defined by the hydrogen bonds: (a) N(1)-D(2)- - -O(3); (b) N(1)-D(3)- - -O(2); (c) N(2)-D(6)- - -O(1); (d) N(1)-D(1)- - -O(2). Contours at 0.05 e/Å^3.

cussed. In a further refinement, the shape of the atomic valence functions is varied by adjustment of a parameter κ such that

$$F(\kappa, S) = f(S/\kappa)$$

where $S = 2 \sin \theta/\lambda$. Values of κ smaller or larger than 1.0 indicate respectively an expansion or contraction of the atomic charge cloud relative to the reference state.[33]

The refinement leads to a small expansion of the carbon and oxygen atoms in comparison with molecule-optimized Slater orbitals,[34] while nitrogen and hydrogen valence shells remain virtually unchanged. The κ values for carbon and oxygen are 0.974 (7) and 0.971 (4) Å, respectively, and correspond to orbital exponents of 1.68 and 2.18 au^{-1} for the Slater-type valence functions. However, relative to isolated atom Hartree-Fock functions the oxygen atom is expanded and the carbon atom *contracted*. This is evident from a second refinement (not further discussed here) in which Hartree-Fock valence form factors were taken as a starting point and also by comparison with the "best single zeta" orbital exponents of Clementi and Raimondi[35] which are 1.59 and 2.23 au^{-1} when averaged over the L-s and L-p shells of the isolated C and N atoms.

The charges calculated from two different refinements—(1) a full refinement varying all positional and thermal parameters and the shape and occupancy of the valence shell and (2) a refinement varying only the shape and occupancy of the valence shell with the positional and thermal parameters fixed at the neutron-refined values—are compared with the charges obtained from two theoretical calculations in Table V.

Table V. Net Atomic Charges

	Experimental		Theoretical	
	κ, STO full refinement	Fixed neutron κ, STO	WR[a]	Sheraga[b]
C(1)	−0.14 (6)	−0.10 (6)	−0.43	−0.12
C(2)	+0.04 (4)	+0.30 (5)	+0.15	+0.45
C(3)	−0.09 (6)	−0.05 (6)	−0.47	−0.08
C(4)	+0.26 (4)	+0.46 (5)	+0.40	+0.50
N(1)	+0.03 (7)	−0.40 (6)	−0.76	−0.29
N(2)	−0.20 (6)	−0.41 (5)	−0.50	−0.34
O(1)	−0.29 (5)	−0.58 (5)	−0.46	−0.38
O(2)	−0.36 (4)	−0.41 (4)	−0.60	−0.50
O(3)	−0.40 (4)	−0.42 (4)	−0.58	−0.50
D(1)	+0.21 (4)	+0.32 (3)	+0.45	+0.26
D(2)	+0.05 (5)	+0.23 (4)	+0.46	+0.26
D(3)	+0.14 (5)	+0.24 (4)	+0.46	+0.26
D(4)	−0.02 (5)	+0.07 (4)	+0.31	+0.06
D(5)	+0.07 (6)	+0.09 (4)	+0.33	+0.06
D(6)	+0.27 (5)	+0.34 (4)	+0.38	+0.18
D(7)	+0.08 (5)	+0.20 (4)	+0.28	+0.06
D(8)	+0.12	+0.10 (4)	+0.28	+0.06
ND_3^+	+0.43	+0.39	+0.61	+0.49
COO^-	−0.50	−0.37	−0.78	−0.50

[a] Reference 5. [b] Reference 6.

The charges presented in Figure 10, when standard deviations are taken into account, are negative on oxygen and nitrogen atoms, not different from zero on the aliphatic carbon atoms, and positive on the carbonyl carbon, the carboxyl carbon, and the ammonio and peptide hydrogen atoms.

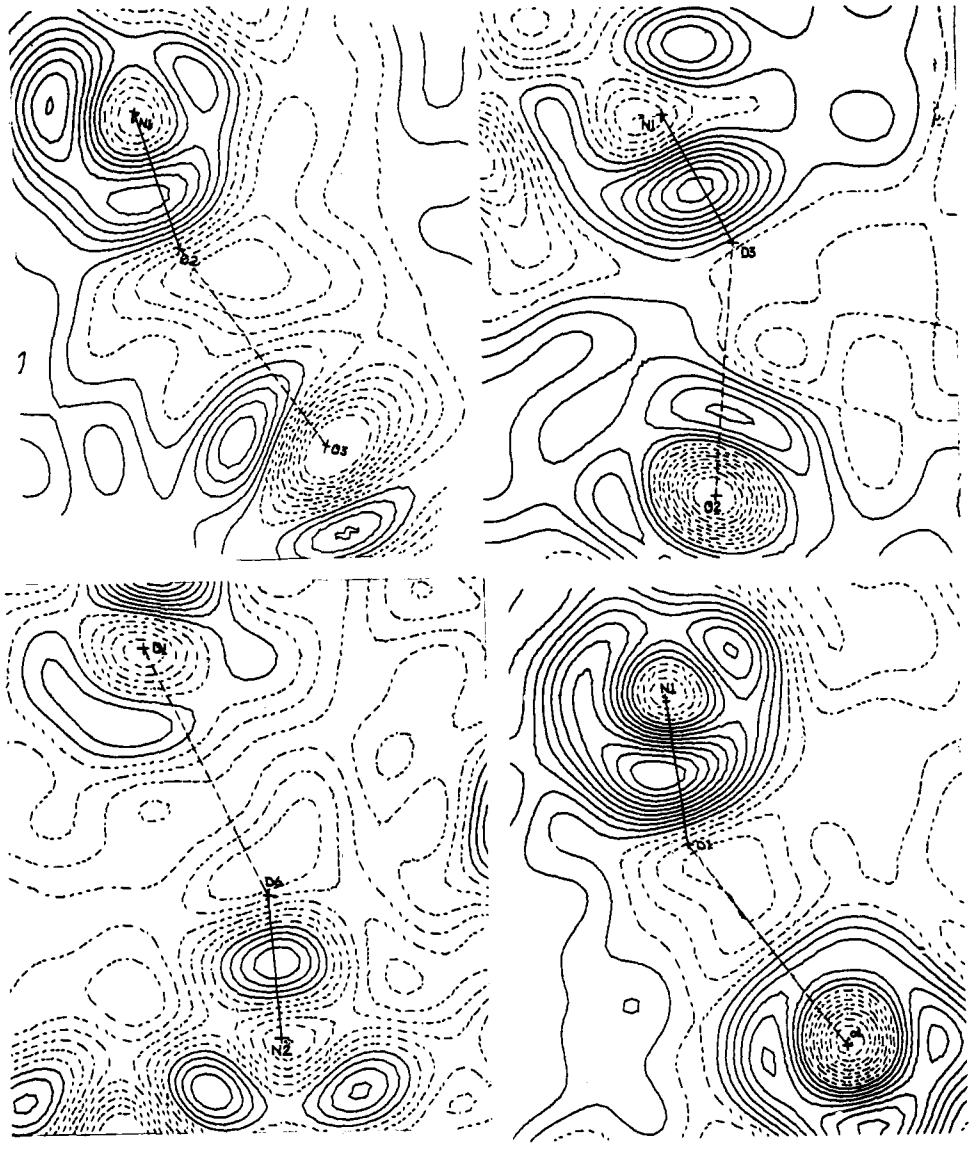

Figure 8. Sections perpendicular to the planes of the hydrogen bonds and containing O- - -D: (a) O(3)- - -D(2); (b) O(2)- - -D(3); (c) O(1)- - -D(6); (d) O(2)- - -D(1).

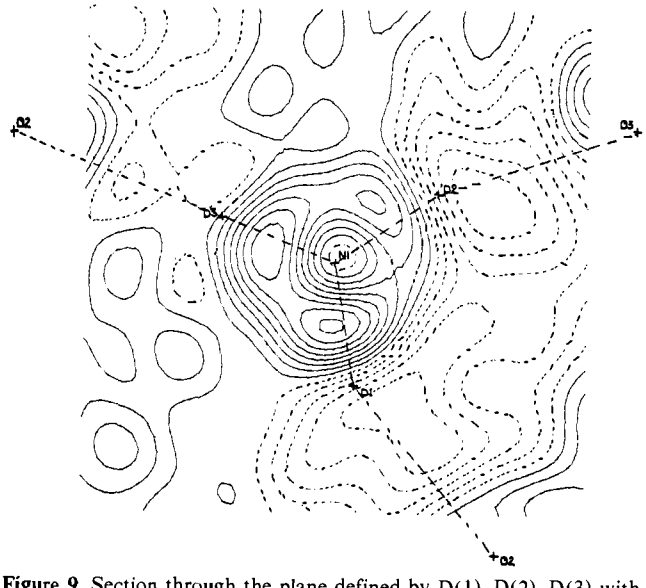

Figure 9. Section through the plane defined by D(1)-D(2)-D(3) with N(1), O(2), O'(2), and O(3) projected onto the plane.

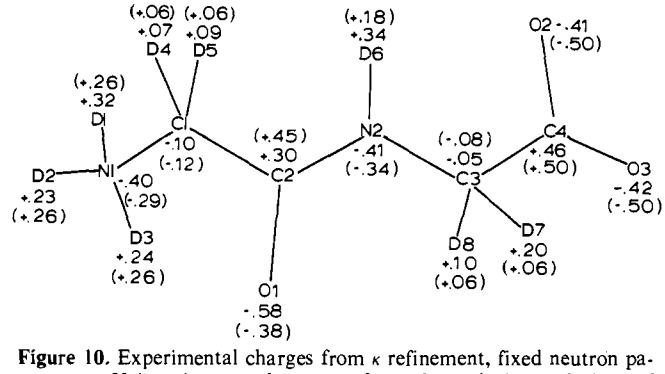

Figure 10. Experimental charges from κ refinement, fixed neutron parameters. Values in parentheses are from theoretical calculations of Sheraga (ref 6).

The charges obtained from the fixed neutron refinement are in almost quantitative agreement with those obtained from the CNDO/2 (ON) calculations of Sheraga, even though theoretical and experimental net atomic charges are not defined in exactly the same manner.[36] This agreement is encouraging and supports the validity of the approximations involved.

Conclusions

The combined X-ray and neutron diffraction technique gives a clear indication of bonding effects in the glycylglycine molecule, especially when deformation densities are considered. The valence density, though appealing from a chemical point of view, is less informative because many effects of interest are masked by the larger total number of electrons in the maps.

The deformation density shows an extension of the peptide C–N bond peak perpendicular to the peptide plane, in agreement with the partial double bond character. The asymmetry of the density in the carboxyl group suggests a polarization due to intramolecular effects or perhaps to hydrogen bonding. There is no buildup of density at the midpoints of the hydrogen bonds, in agreement with the electrostatic model for this interaction. N–D vectors point toward the lone pairs on the acceptor atoms rather than to the atomic centers. The net charges on the COO^- and NH_3^+ groups are found to be about -0.4 to -0.5 and $+0.4$ electrons, respectively; thus, any discussion of molecular structure of polypeptides and proteins assuming integral charges on these groups must be modified.

The accuracy of the present study is limited primarily by the neutron diffraction measurements, which should be repeated if greater resolution is desired. Data collection at low temperature would further enhance the detail in the density maps.[1,19] Glycylglycine crystallizes in three polymorphic modifications of differing molecular conformation.[7] A study of the relation between the electron density and the conformation of the molecule would also be of considerable interest.

Acknowledgments. The authors thank Drs. Paul and Sabine for supplying the crystal used for X-ray data collection and Dr. R. H. Blessing for experimental assistance. Partial support of the National Science Foundation is gratefully acknowledged.

References and Notes

(1) P. Coppens, *Acta Crystallogr., Sect. B*, **30**, 255–261 (1974).
(2) P. Becker, P. Coppens, and F. K. Ross, *J. Am. Chem. Soc.*, **95**, 7604–7609 (1973).
(3) P. Coppens, *MTP Int. Rev. Sci.: Phys. Chem.*, in press.
(4) H. C. Freeman, G. L. Paul, and T. M. Sabine, *Acta Crystollogr., Sect. B*, **26**, 925–932 (1970).
(5) J. A. Ryan and J. L. Whitten, *J. Am. Chem. Soc.*, **94**, 2396–2400 (1972).
(6) F. A. Momany, L. M. Carruthers, and H. A. Sheraga, *J. Phys. Chem.*, **78**, 1621–1630 (1974).
(7) A. B. Biswas, E. W. Hughes, B. D. Sharma, and J. N. Wilson, *Acta Crystallogr., Sect. B*, **24**, 40–50 (1968).
(8) W. R. Busing and H. A. Levy, *Acta Crystallogr.*, **22**, 457–464 (1967).
(9) R. Blessing, P. Coppens, and P. Becker, *J. Appl. Crystallogr.*, **7**, 488–492 (1974).
(10) R. F. Stewart, E. R. Davidson, and W. T. Simpson, *J. Chem. Phys.*, **42**, 3175–3187 (1965).
(11) (a) F. L. Hirshfeld and D. Rabinovich, *Acta Crystallogr., Sect. A*, **29**, 510–513 (1973); (b) P. Coppens and W. C. Hamilton, *Acta Crystallogr., Sect. B*, **24**, 925–929 (1968).
(12) The X-ray structure factor table may be obtained from the authors on request.
(13) The Neutron Diffraction Commission, *Acta Crystallogr., Sect. A*, **25**, 391–392 (1969).
(14) P. Coppens, T. M. Sabine, R. G. Delaplane, and J. A. Ibers, *Acta Crystallogr., Sect. B*, **25**, 2451–2458 (1969).
(15) P. P. M. Groenewegan, J. Zeevalkink, and D. Feil, *Acta Crystallogr., Sect. A*, **27**, 487–491 (1971).
(16) P. Coppens, *Isr. J. Chem.*, **10**, 85–91 (1972).
(17) W. F. Cooper, F. K. Larsen, P. Coppens, and R. F. Giese, *Am. Mineral*, **58**, 21–31 (1973).
(18) F. K. Winkler and J. D. Dunitz, *J. Mol. Biol.*, **59**, 169–182 (1971).
(19) P. Coppens and A. Vos, *Acta Crystallogr., Sect. B*, **27**, 146–158 (1971).
(20) H. Irngartinger, L. Leiserowitz, and G. M. J. Schmidt, *J. Chem. Soc. B*, 497–504 (1970).
(21). R. B. Helmholdt, A. F. J. Ruysink, J. Reynaars, and G. Kemper, *Acta Crystallogr., Sect. B*, **28**, 318–319 (1972).
(22) C. A. Coulson, *Mem. Soc. R. Sci. Liege, Collect. 8°*, **6(2)**, 143–162 (1971).
(23) R. F. Stewart, *J. Chem. Phys.*, **48**, 4882–4889 (1968).
(24) E. D. Stevens, Ph.D. Thesis, University of California, Davis, Calif., 1973.
(25) J. Almlöf, Å. Kvick, and J. O. Thomas, *J. Chem. Phys.*, **59**, 3901–3910 (1973).
(26) J. C. Taylor and T. M. Sabine, *Acta Crystallogr., Sect. B*, **28**, 3340–3351 (1972).
(27) P. A. Kollman and L. C. Allen, *J. Chem. Phys.*, **52**, 5085–5094 (1970).
(28) M. Dreyfus, B. Maigret, and A. Pullman, *Theor. Chim. Acta*, **17**, 109–119 (1970).
(29) L. Leiserowitz and G. M. J. Schmidt, *J. Chem. Soc. A*, 2372–2382 (1969).
(30) R. F. Stewart, *J. Chem. Phys.*, **53**, 205–213 (1970).
(31) P. Coppens, D. Pautler, and J. F. Griffin, *J. Am. Chem. Soc.*, **93**, 1051–1058 (1971).
(32) R. F. Stewart, *J. Chem. Phys.*, **51**, 4569–4580 (1969).
(33) P. Coppens, unpublished results.
(34) W. J. Hehre, R. F. Stewart, and J. A. Pople, *J. Chem. Phys.*, **51**, 2657–2664 (1969).
(35) E. Clementi and D. L. Raimondi, *J. Chem. Phys.*, **38**, 2686–2691 (1963).
(36) P. Coppens, *Trans. Am. Crystallogr. Assoc.*, **8**, 93–108 (1972).